Stochastic entropies and fluctuation theorems for a generic 1D KPZ system: internal and external dynamics

Miguel A. Rodríguez[1], Rafael Gallego[2] and Horacio S. Wio[3]

[1] Instituto de Física de Cantabria (IFCA), CSIC-UNICAN, E-39005 Santander, Spain
[2] Departamento de Matemáticas, Universidad de Oviedo, Campus de Gijón, E-33203 Gijón, Spain
[3] Instituto de Física Interdisciplinar y Sistemas Complejos (IFISC), CSIC-UIB, E-07122 Palma de Mallorca, Spain

PACS 89.75.Da – First pacs description
PACS 05.40.-a – Second pacs description
PACS 05.45.Tp – Third pacs description

Abstract –In a recent numerical study, we have analyzed the stochastic entropies and fluctuation theorems in a 1D KPZ system. Such a study only considered saturated fluctuations around the spatial mean value of the interface. In this way stationary solutions exist and besides, with some particular discrete version, those solutions are exactly known. In this paper we extend these previous results in two ways. On the one hand, the dynamics of the spatial mean value is taken into account. We then distinguish between the entropies associated with internal fluctuations (of the interface around the spatial mean), and external fluctuations (of the spatial mean around the sample mean) dynamics. On the other hand a broader region of parameters is analysed. Two distinct behaviors appear depending on whether after saturation the system overcomes the Edward-Wilkinson crossover towards the KPZ regime or not.

Introduction. – One of the most emblematic, and also non-trivial, model of out of equilibrium extended systems corresponds to the Kardar-Parisi-Zhang (KPZ) equation [1]. It was introduced within the description of growing of rough surfaces [1,2]. In its more generic one dimensional form reads

$$\frac{\partial h(x,t)}{\partial t} = \mu\partial_x^2 h(x,t) + \frac{\lambda}{2}(\partial_x h(x,t))^2 + \xi(x,t), \qquad (1)$$

where $h(x,t)$ is the height of a given interface growing under the effect of a combined action of diffusive and non-linear forces and simultaneously driven by an uncorrelated space-time Gaussian noise ($\langle\xi(x,t)\xi(x',t')\rangle = 2D\delta(x-x')\delta(t-t')$). Its linear version, i.e. $\lambda = 0$, corresponds to the Edwards-Wilkinson (EW) equation [3].

Since its introduction [1] it has been the subject of a large number of studies, both analytic and numerical, exploiting a wide variety of techniques [2–5], even including functional approaches [6–8]. More recent interest has focused on the possibility of finding some exact results as well as exploiting the very rich mathematical connection with other far related problems [2,9–12].

Despite its intrinsic interest, studies of the statistical behavior of entropy and entropy production in this system are scarce [13]. Among the few known cases, a deposition model whose dynamics belongs to the KPZ universality class has been analyzed [14], in [15,16] a field theoretical approach to study thermodynamic uncertainty relations was applied and in [17,18] a direct and tight relation among entropy production and the non-equilibrium potential for the KPZ equation is presented.

In a recent work [19], and due to the fact that the usual time-independent solution of the associated Fokker-Planck equation is not strictly a stationary probability since it cannot be normalized, we resorted to transform the usual variables to new ones with zero spatial mean. We have exploited discrete representations in order to prove statistical properties of entropies, and have performed direct numerical tests of the fluctuation theorems. But only saturated fluctuations around the spatial mean value of the interface were considered. Within this framework, stationary solutions exist and, for particular discrete representations, those solutions could be exactly known. Here, we have extended those results in a couple of directions. On one hand we considered the dynamics of the spatial mean value, distinguishing between the entropies associated with internal fluctuations of the interface around the spatial mean, and the external fluctuations of the spatial

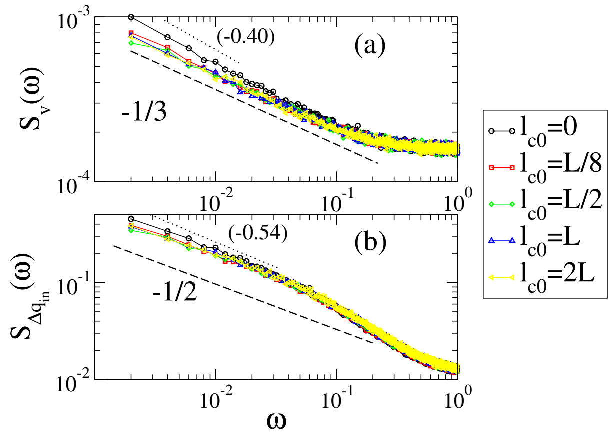

Fig. 1: PSD of the centre of masses velocity v (a) and entropy rate (b) fluctuations of an interface in the KPZ regime ($\mu = 0.1$) when the initial condition is an interface with correlation length l_{c0}. The initial correlation ranges from a flat to a well saturated interface. We take $l_c(t) = 3t^{3/2}$, $L = 256$, 1000 samples, and parameters $\lambda = 1$,$D = 0.01$.

mean around the sample mean dynamics. On the other hand, we analysed a broader region of parameters. Our results show that two different behaviors could arise depending on whether after saturation the system overcomes the EW crossover towards the KPZ regimen or not. In the first case, the behavior of fluctuations is dominated by the diffusive term whereas in the second, the behavior corresponds to a genuine KPZ regime.

We consider that, from the point of view of growing processes, the present study offers a novel perspective for the analysis of such phenomena, and particularly for the study of the emblematic KPZ dynamics. First steps on this direction are the above mentioned connection between entropy production and the non-equilibrium potential for the KPZ equation [17,18] . We also consider that it opens the door for an stochastic thermodynamic analysis of non-equilibrium extended systems that present both, internal and external fluctuations, helping to understand the role that each one could play. The use of a KPZ system to check a thermodynamic relation [15,16] is a recent example to see the potentiality of this interplay.

Internal and external fluctuations. – Due to the non-linearity of the KPZ equation, an interesting fact is the coupling between the internal fluctuation modes and the center of mass motion of the interface [5]. Such a coupling arises when the evolution equations of the internal fluctuations $z(x,t) = h(x,t) - \overline{h(t)}$ and the center of mass $\overline{h}(t)$ are considered:

$$\frac{\partial z(x,t)}{\partial t} = \mu \partial_x^2 z(x,t) + \frac{\lambda}{2}\left(\partial_x z(x,t)\right)^2 - \frac{\lambda}{2}\overline{\left(\partial_x z(x,t)\right)^2} + \xi(x,t) \qquad (2)$$

$$\dot{\overline{h}}(t) = \frac{\lambda}{2}\overline{\left(\partial_x z(x,t)\right)^2} + \overline{\xi(x,t)}. \qquad (3)$$

From now on an overline $\overline{F(x,t)}$ will indicate spatial average whereas the sample average will be denoted by angular brackets $\langle F(x,t)\rangle$. Hence, while internal fluctuations are independent of the external ones, fluctuations of the center of mass are completely dependent on the internal fluctuations. The internal fluctuation dynamics is described by a well-known dynamical scaling theory, introducing two universal exponents that should be taken into account: the growth of the correlation length $l_c(t) \sim t^{1/z}$ and the interface width $W(t) \sim t^{\beta}$ [3]. In a finite system of size L the interface saturates in a time t_s such that $l_c(t_s) \sim L$, and the width in the saturation regime scales with the system size according to $W(L) \sim L^{\alpha}$, with $\alpha = z\beta$. Here z is the so called dynamical exponent whereas β is the growth exponent. A typical evolution of an interface following the KPZ equation and having a flat initial condition exhibits two growth regimes. The first one, known as the EW regime, is dominated by the linear term of the equation and is characterized by exponents $z = 2$, $\beta = 1/4$, while the second, the genuine KPZ regime, has exponents $z = 3/2$, $\beta = 1/3$. Hence, there should be a crossover time and a crossover length separating both regimes. Thus, a given system with a size smaller than this crossover length only shows diffusive correlations with $z = 2$, but with a mean velocity typical of a KPZ system. We then say that this is a KPZ finite system in the EW regime. On the contrary, systems with sizes much larger than the crossover length exhibit fluctuations typical of the genuine KPZ regime.

Another important feature of the KPZ equation is that some relevant quantities can be written in terms of the parameters of the equation. A useful example is, for instance, the crossover time, that in terms of parameters reads [5]

$$t_{\rm cross} = 8\pi^{-3} c_2^{-6} \mu^5 D^{-2} |\lambda|^{-4}, \qquad (4)$$

c_2 being a universal amplitude with value $c_2 \approx 0.40$.

In addition, the strong dependence of the external fluctuations on the internal modes determines the statistics of this external process in terms of exponents as well as parameters. The center of mass moves with a mean velocity

$$\langle \dot{\overline{h}}(t)\rangle = \frac{D\lambda}{4\mu}\left(\frac{1}{a} - \frac{1}{L}\right) + O(1/L^2), \qquad (5)$$

a and L being respectively the lattice cut-off and the system size [5]. It is worth noting that this explicit dependence on the cut-off means that this velocity is not a universal coefficient, so it will be dependent on the discrete version one uses. Fluctuations of the velocity $\delta\dot{\overline{h}}(t) = \dot{\overline{h}}(t) - \langle\dot{\overline{h}}(t)\rangle$ follow a stationary process that is uncorrelated in the EW regime and correlated in the KPZ regime [5]. In a finite system, fluctuations become again uncorrelated after saturation. The power spectral density (PSD) of this process in the correlated regime scales with the system size L and frequency ω as $S_v(\omega, L) \sim L^{-1}\omega^{-1/3}$. This process was considered an example of the ubiquity of $1/f$ noise appearing, in this case, in the interface growth

[20]. Being more precise it is better to use the classification introduced in [21] in which it is a stationary correlated process with spectral exponent $\alpha_s = -1/3$ and global exponent $\alpha_g = 0$. The center of mass, $\overline{h}(t)$, which is the cumulative process of the velocity, then follows a self-affine process with the same scaling for the system size and a Hurst exponent given by $H = \alpha_s + 1$. Then the variance $\sigma^2_{\overline{h}} = \langle \delta\overline{h}(t)^2\rangle$ follows a diffusive behavior as $\sigma^2_{\overline{h}}(L,t) = Dt/L$ in the EW regime and it scales as

$$\sigma^2_{\overline{h}}(L,t) \sim Lg(t/L^{3/2}) \tag{6}$$

in the KPZ regime, with $g(u) \sim u^{4/3}$ before saturation ($u \ll 1$) and $g(u) \sim u$ after saturation ($u \gg 1$). It is worth remarking that the scaling forms of the external fluctuations shown here can be deduced from the scaling of the correlation of internal fluctuations in a stationary regime [5, 20]. However, nothing is known when the interface departs from an unsaturated interface where the internal modes are still growing. Numerical simulations shown in Fig. 1(a) indicate that correlations of the velocity are independent of the interface initial degree of correlation. Only when the initial state is a flat interface one observes a small difference in the PSD producing a slight increment in the spectral exponent.

Discrete equations. – Any discrete version of Eqs. (1,2) can be written as a Langevin equation of the form

$$\dot{y}_i(t) = Y_i(\mathbf{y}) + \xi_i(t), \tag{7}$$

with $Y_i(\mathbf{y} + k\mathbf{u}) = Y_i(\mathbf{y})$, k being an arbitrary constant and $\mathbf{u}$ the unit vector, and noise correlations

$$\langle \xi_i(t)\xi_j(s)\rangle = \frac{2D}{a}\delta_{i,j}\delta(t-s), \tag{8}$$

with a, as indicated, being the spatial cutoff, $N = L/a$ and $i \in [1, N]$. For equations like (2), with interfaces with null mean velocity, it is necessary to also add the condition $\overline{\mathbf{Y}} = 0$. Such Langevin equations admit a Fokker-Planck equation for the probability density $P(\mathbf{y}, t)$

$$\frac{\partial P(\mathbf{y},t)}{\partial t} = -\sum_{i=1}^{N}\frac{\partial}{\partial y_i}(Y_i P(\mathbf{y},t)) + \frac{D}{a}\sum_{i=1}^{N}\frac{\partial^2}{\partial y_i^2}P(\mathbf{y},t), \tag{9}$$

and also a functional form of the probability for a given path [22, 23]

$$P[\mathbf{y}(s)|\mathbf{y}(t_i)] \sim \exp\left[-\frac{a}{4D}\int_{t_i}^{t_f} ds \sum_{i=1}^{N}(\dot{y}_i(s) - Y_i(\mathbf{y}))^2\right], \tag{10}$$

t_i and t_f being respectively the initial and final time of the path. With these elements at hand, one can easily apply a stochastic thermodynamics theory, defining the interchange entropy for a trajectory $[\mathbf{y}(s)]$ as the logarithm of the ratio between the probabilities of the forward to backward trajectories indicated by $\overleftarrow{\mathbf{y}(s)}$

$$\Delta s_m[\mathbf{y}(s)] = \log\left(\frac{P[\mathbf{y}(s)|\mathbf{y}(t_i)]}{P[\overleftarrow{\mathbf{y}(s)}|\mathbf{y}(t_f)]}\right), \tag{11}$$

and the total entropy production as

$$\Delta s_{\mathrm{tot}}[\mathbf{y}(s)] = \Delta s_m[\mathbf{y}(s)] - \log\left[\frac{P(\mathbf{y}(t_f), t_f)}{P(\mathbf{y}(t_i), t_i)}\right]. \tag{12}$$

Taking the separation between external and internal processes as: $\mathbf{y}(t) = \overline{y}(t)\mathbf{u} + \mathbf{z}(t)$, where we have used the unit vector $\mathbf{u}$ to keep the vector notation and substituting in Eqs. (11,12), considering as in [19] the linear and nonlinear parts of the force $Y_i = \mu\Gamma_i + \frac{\lambda}{2}\Phi_i$, integrating the linear part using $\Gamma_i = -\frac{\partial U}{\partial y_i}$, and separating the contributions due to internal and external contributions, we have

$$\Delta s_m^{\mathrm{in}}[\mathbf{z}(\mathbf{s})] = \frac{a\lambda}{2D}\int_{t_i}^{t_f} ds \sum_i \dot{z}_i(s)\Phi_i(\mathbf{z}(s)) - \frac{a\mu}{D}\left[U(\mathbf{z}(t_f)) - U(\mathbf{z}(t_i))\right], \tag{13}$$

$$\Delta s_m^{\mathrm{ex}}[\overline{\mathbf{y}}(s), \mathbf{z}(\mathbf{s})] = \frac{a\lambda}{2D}\int_{t_i}^{t_f} ds\, \dot{\overline{\mathbf{y}}}(s)\sum_i \Phi_i(\mathbf{z}(s)). \tag{14}$$

Here we have assumed that $\sum_i \Gamma_i = 0$, $\Gamma_i(\mathbf{y}) = \Gamma_i(\mathbf{z})$ and $\Phi_i(\mathbf{y}) = \Phi_i(\mathbf{z})$. We see how the entropies of the external process depend on the fluctuations of the internal system, but not on the contrary. With the total entropy production we operate in the same way, taking into account that $P(\mathbf{y}, t) = P(\mathbf{z}, t)W(\overline{\mathbf{y}}|\mathbf{z}, t)$.

$$\Delta s_{\mathrm{tot}}^{\mathrm{in}}[\mathbf{z}(\mathbf{s})] = \Delta s_m^{\mathrm{in}} - \log\left[\frac{P(\mathbf{z}(t_f), t_f)}{P(\mathbf{z}(t_i), t_i)}\right], \tag{15}$$

$$\Delta s_{\mathrm{tot}}^{\mathrm{ex}}[\overline{\mathbf{y}}(s), \mathbf{z}(\mathbf{s})] = \Delta s_m^{\mathrm{ex}} - \log\left[\frac{W(\overline{\mathbf{y}}(t_f)|\mathbf{z}, t_f)}{W(\overline{\mathbf{y}}(t_i)|\mathbf{z}, t_i)}\right]. \tag{16}$$

The conditioned probability $W(\overline{\mathbf{y}}|\mathbf{z}, t)$ obeys a backward Fokker-Planck equation (see Supplementary Material SM1). Note, as seen in [19], that an expression for the probability $P(\mathbf{z}, t)$ of the internal part is only known in the stationary case and for special discretizations. Even a numerical evaluation is not possible. Therefore, for the computation of total entropies we restrict ourselves to the case of stationary internal fluctuations, that is, when the interface becomes saturated and then $P(\mathbf{z}) \sim \exp(-\frac{a\mu}{D}U(\mathbf{z}))$. If additionally we approximate the conditional probability $W(\overline{\mathbf{y}}(t)|\mathbf{z}, t)$ with a Gaussian distribution of mean $\langle\overline{\mathbf{y}}(t)\rangle$ and dispersion $\sigma_{\overline{y}}(t)$, we obtain numerically tractable expressions for the total entropy production as:

$$\Delta s_{\mathrm{tot}}^{\mathrm{in}}[\mathbf{z}(\mathbf{s})] = -\frac{a\lambda}{2D}\int_{t_i}^{t_f} ds \sum_i \dot{z}_i(s)\Phi_i(\mathbf{z}(s)), \tag{17}$$

$$\Delta s_{\mathrm{tot}}^{\mathrm{ex}}[\overline{\mathbf{y}}(s), \mathbf{z}(\mathbf{s})] = \frac{a\lambda}{2D}\int_{t_i}^{t_f} ds\, \dot{\overline{\mathbf{y}}}(s)\sum_i \Phi_i(\mathbf{z}(s)) + \log\left(\frac{\sigma_{\overline{y}}(t_f)}{\sigma_{\overline{y}(t_i)}}\right) + \frac{\delta\overline{y}(t_f)^2}{2\sigma^2_{\overline{y}}(t_f)} - \frac{\delta\overline{y}(t_i)^2}{2\sigma^2_{\overline{y}}(t_i)}. \tag{18}$$

Conversely, computation of interchange entropies by means of numerical simulations is always possible exploiting equations (13) and (14). Finally, since we are interested in the statistics of these entropies, we define in each case their probability densities as: $P(r_{\rm in}) = \langle \delta(r_{\rm in} - \Delta s_m^{\rm in})\rangle$, $P(r_{\rm ex}) = \langle \delta(r_{\rm ex} - \Delta s_m^{\rm ex})\rangle$, $P(q_{\rm in}) = \langle \delta(q_{\rm in} - \Delta s_{\rm tot}^{\rm in})\rangle$ $P(q_{\rm ex}) = \langle \delta(q_{\rm ex} - \Delta s_{\rm tot}^{\rm ex})\rangle$, that can be computed numerically as normalized histograms of the above defined functional.

Numerical analysis. – As in [19], we simulate the Langevin equation with periodic boundary conditions and pre-point time discretization

$$y_i(t_{j+1}) = y_i(t_j) + \nu Y_i(\mathbf{y}(t_j)) + \sqrt{\frac{2D\nu}{a}}\,\xi_{i,j}, \qquad (19)$$

$\xi_{i,j}$ being independent normalized Gaussian noises. We take $\nu = 0.01$ and $a = 1$ as time and space steps.

We have first analysed the role of our discrete versions in the calculation of entropies. This is important since different discretizations produce distinct results in amplitudes, but not in exponents. The KPZ equation is a singular stochastic partial differential equation that needs some kind of regularization. This is an interesting mathematical problem [12]. A physically acceptable regularization is to use a cutoff in the spatial or spectral scale. In this way some results, such as amplitudes of entropies and velocities, are explicitly dependent on the value of the cutoff.

The key point is to find discrete systems with a probability density $P(\mathbf{z})$ equal or close to the exact solution of the stationary Fokker-Planck equation. Taking for the linear term the standard diffusive term, $\Gamma_i(\mathbf{y}) = a^{-2}(y_{i+1} + y_{i-1} - 2y_i)$, and keeping the condition $\Gamma_i = -\frac{\partial U(\mathbf{y})}{\partial y_i}$, we obtain two possibilities for the potential $U^{\pm}(\mathbf{y}) = \frac{1}{2a^2}\sum_j (y_{j\pm1} - y_j)^2$ that are equivalent assuming cyclic boundary conditions. If we want exact solutions of the time independent Fokker-Planck equation of the form $P(\mathbf{y}) = \exp(-\frac{a\mu}{D}U^{\pm}(\mathbf{y}))$, we need to use a nonlinear term with the condition $\sum_{i=1}^{N}\left(\frac{\partial \Phi_i}{\partial y_i} + \Phi_i\Gamma_i\right) = 0$. The simpler case is $\Phi_i^{\rm exact}(\mathbf{y}) = \frac{1}{3a^2}[(y_{i+1}-y_i)^2 + (y_{i+1}-y_i)(y_i - y_{i-1}) + (y_i - y_{i-1})^2]$ [24]. However we have checked other possibilities with the conclusion that they are so good approximations that become indistinguishable from the exact result. This occurs, for instance, for the nonlinear terms $\Phi_i^{+}(\mathbf{y}) = \frac{1}{a^2}(y_{i+1} - y_i)^2$, $\Phi_i^{-}(\mathbf{y}) = \frac{1}{a^2}(y_{i-1} - y_i)^2$ and $\Phi_i^{\rm sym}(\mathbf{y}) = \frac{1}{4a^2}(y_{i+1} - y_{i-1})^2$. In [19] other possibilities for discrete representation with non standard forms of Γ were explored. Here, and for the sake of having a broader interval of parameters with numerical stability, we avoid these type of discrete versions. In fact, the case with the nonlinear term $\Phi^{\rm sym}$ provides the broadest interval of stability, which allows to reach the genuine KPZ regime with relatively small system sizes. Taking as in [19] two extreme values of parameters λ and D, labeled as LD1, $\lambda = 0.1$, $D = 1$, and LD2, $\lambda = 1$, $D = 0.01$, we find numerical stability for $\mu > 0.4$ in the cases $\Phi^{\pm}$ and for $\mu > 0.1$ when using $\Phi^{\rm sym}$. Estimating that the system size will allow to overcome the EW regime as $L_{\rm cross} = \sqrt{\frac{288\mu t_{\rm cross}}{\pi}}$, [5,16] and using (4), we have $L_{\rm cross} \sim 7.6$ for $\mu = 0.1$ and $L_{\rm cross} \sim 486$ for $\mu = 0.4$. Using systems of no more than 1024 space points we need values of $\mu << 0.5$ to overcome the EW crossover. Then is clear that the KPZ regime can be well established, $L_{\rm coss} << L$, only with the use of the nonlinear term $\Phi^{\rm sym}$.

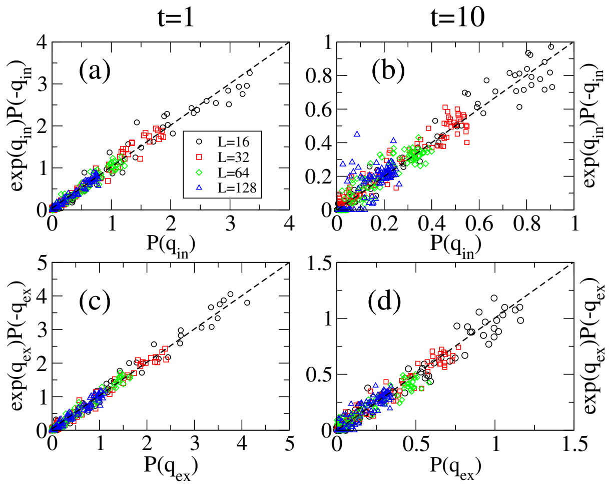

Fig. 2: Direct checking of the detailed fluctuation theorem. Upper row: Plot of $\exp(q_{\rm in})P(-q_{\rm in})$ vs. $P(q_{\rm in})$ for $t = 1$ (a) and $t = 10$ (b). Lower row: Plot of $\exp(q_{\rm ex})P(-q_{\rm ex})$ vs. $P(q_{\rm ex})$ for $t = 1$ (c) and $t = 10$ (d). The model is KPZ with the symmetric discretization ($\Phi^{\rm sym}$) and parameters $\mu = \lambda = 1$, $D = 0.01$.

In our numerical simulations, we start with saturated interfaces when calculating total entropies, and with flat interfaces in the case of interchange entropies. This initial interfaces, which have a zero spatial mean $\mathbf{y}(0) = \mathbf{0}$, are evolved using (19) up to a time t_i, the initial time of the paths used to compute the entropies. Paths are evaluated in intervals (t_i, t_f) using formulas (13,14) for exchange entropies and (17,18) for total entropies. All our results will be presented as functions of the path time spanned $t = t_f - t_i$, avoiding any explicit mention of t_i since it is irrelevant in our discussions. We take in all simulations $t_i = 2$ to avoid divergences that would appear if we took $t_i = 0$ in (18).

A direct check of the detailed fluctuation theorem. In general, the detailed fluctuation theorem $P(q) = e^q P(-q)$ holds for stationary non-equilibrium systems as is our case of internal fluctuations with $P(q_{\rm in})$ [13, 19]. For non-stationary systems, as is the case of external fluctuations with $P(q_{\rm ex})$, one would expect the failure of such detailed theorem, mainly due to the asymmetry in the initial and final probability densities (see Supplementary Material SM2). However, as shown in Fig. 2, the detailed fluctuation theorem also holds in the case of external fluctuations, the reason being that fluctuations of the external entropy are dominated by the stationary dynamics of the internal

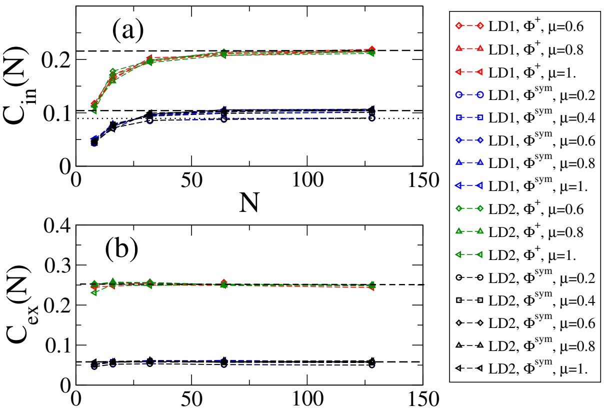

Fig. 3: Dimensionless parameter $C_{\text{in(ex)}}(N)$ in the cases of internal (a) and external (b) fluctuations for several sets of system parameters. $C_{\text{in(ex)}}(N)$ depends on the discretization, reaching a saturation value represented by a dashed line. These saturation values are $(C_{\text{ex}}, C_{\text{in}}) = (0.248, 0.216)$ for the Φ^+ discretization and $(C_{\text{ex}}, C_{\text{in}}) = (0.056, 0.105)$ for the Φ^{sym} discretization. Note that in the case of symmetrical discrete representation, $C_{\text{in}}(N)$ is slightly smaller in the KPZ regime, with $\mu = 0.2, 0.4$ (dotted line) than in the EW regime with $\mu > 0.4$.

modes given by the first term in Eq. (18). In the cases presented in Fig. 2 the second term contributes less than 0.3 per cent to the total value.

In Fig. 2 we plot the cases $t = 1$ and $t = 10$ using histograms with 100 bins and 10000 samples. The figure shows how the detailed fluctuation theorem clearly holds for the given parameters for both internal and external fluctuations. Note that this direct checking is only possible for short times and good sample statistics in order to keep the statistical errors of the negative part of the histogram small enough. For longer times the stationary dynamics becomes even more dominant since the first term of Eq. (18) grows linearly with time whereas the other terms only add a logarithmic correction in time. So the theorem should also hold for long times. Similar results are obtained for any set of parameters belonging to the interval of numerical stability.

Interchange and total entropy productions.. Following the description given in [19] we first analyze the mean values of entropies, defined as

$$Q_{\text{in(ex)}}(t) = \int q_{\text{in(ex)}} P(q_{\text{in(ex)}}) dq_{\text{in(ex)}}, \tag{20}$$

$$R_{\text{in(ex)}}(t) = \int r_{\text{in(ex)}} P(r_{\text{in(ex)}}) dr_{\text{in(ex)}}. \tag{21}$$

From (13) and (14) one easily sees that $Q_{\text{in}}(t) = R_{\text{in}}(t)$ and $Q_{\text{ex}}(t) = R_{\text{ex}}(t) + \log\left(\frac{\sigma_{\overline{y}}(t+t_i)}{\sigma_{\overline{y}}(t_i)}\right)$. Numerical simulations of these quantities indicate that the asymptotic values are reached in a very short time, showing a perfect linear dependence on time. This fact, together with the extensive character of entropies, suggest the introduction

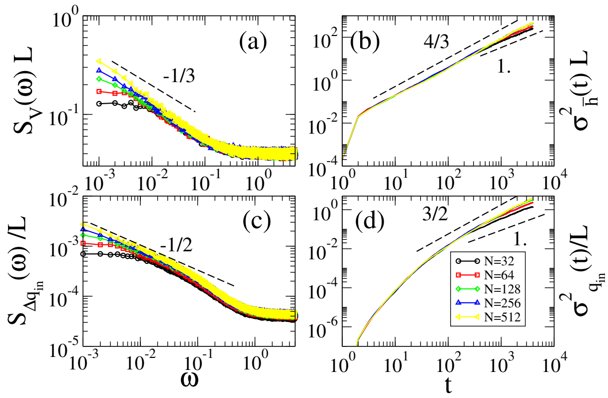

Fig. 4: PSDs of the spatial averaged velocity (a) and the total entropy rate of internal fluctuations (c) for KPZ systems with distinct sizes. For the sake of comparison we plot on the right column the variance of their corresponding cumulative processes, the spatial averaged height (b) and the total entropy production (d). Parameters of the KPZ equations are chosen to keep the system in a genuine KPZ regime, namely $\lambda = 1$, $D = 0.01$, $\mu = 0.1$. Dashed lines are depicted to guide the eye.

of $\rho_{\text{in(ex)}}$, the entropy production density rate, as:

$$Q_{\text{in(ex)}} \sim R_{\text{in(ex)}} = \rho_{\text{in(ex)}} aNt. \tag{22}$$

From a numerical analysis we find that:

$$\rho_{\text{in(ex)}} = C_{\text{in(ex)}}(N) \frac{D\lambda^2}{a^2\mu^2}. \tag{23}$$

As shown in Fig. 3 $C_{\text{in(ex)}}$ is a dimensionless parameter that varies with N, the type of discretization and the regime within which the system is evolving. It grows with the size N until reaching a saturated value at relatively small sizes (~ 30 for C_{in} and ~ 5 for C_{ex}). It is smaller for the symmetrical discretization case (Φ^{sym}), since it is numerically more stable than the asymmetrical case (Φ^+). Finally, a small difference in the asymptotic value can be seen in the figure when the parameters lead the system to a change in the regime. This difference could be due to a systematic numerical error of about 10% that appears in the calculation of entropies as reported in [16].

Variance of entropies. In a finite system it is necessary to carefully distinguish between the ensemble average and the spatial average, as shown in [5] for the interface height. This also applies to any other spatially averaged quantities, such as the entropies defined in this paper, or the equivalent non-equilibrium potentials. In fact, fluctuations of both the spatially averaged height and the entropies, around their ensemble average, behave similarly. In the EW regime both of them present diffusive behavior, while they are super-diffusive in the KPZ regime. Also, both exhibit diffusive behaviour after saturation and the degree of correlation of their initial conditions turns out to be irrelevant in their evolution, as shown in Fig. 1. In Fig. 4 we show the PSD scaling of the fluctuations of the

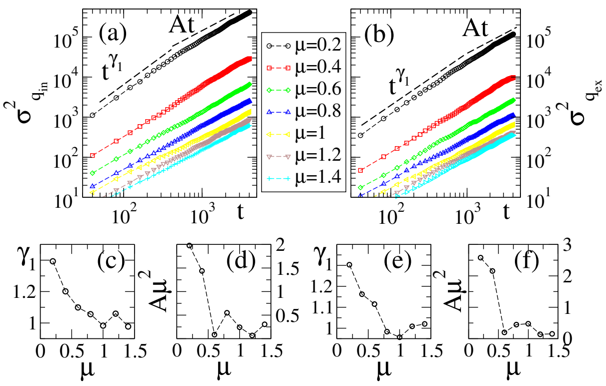

Fig. 5: Variances of total entropies (of the internal (a) and external (b) fluctuations) as a function of time for several values of μ ranging from $\mu = 1.4$ (diffusive correlations, EW regime) to $\mu = 0.2$ (KPZ regime). Between both values one can observe the effect of a crossover in the time exponent before saturation (c),(e) and in the growth constant after saturation (d),(f).

instantaneous velocity and the entropy production rate. They are stationary correlated processes with spectral exponents [21] $\alpha_s = -1/3$ (Fig.4 (a)) and $\alpha_s = -1/2$ (Fig.4 (c)). In the first column of Fig. 4 we show the same spectra but now scaled with the system size. The second column of the figure shows the scaling of the variance of the cumulative processes which are the height and entropy fluctuations. The scaling exponents can be corroborated against the growth exponent of the variance that is equal to $2(\alpha_s + 1)$. Note that the change of regime in the analysis of stationary processes, which goes from a $1/\omega^{2\alpha_s+1}$ to a flat spectrum, is more evident than for their cumulative processes, that are sometimes difficult to be appreciated. Since in this paper we are mainly interested in the statistic of entropies, we present our results in terms of the mean (last subsection) and the variance of entropies.

The first analysis deals with the detection of the distinct regimes of fluctuation. To this end we show in Fig. 5 the variances of total entropy production (of both internal and external fluctuations) as a function of time and for several values of parameters. We see that in some parameter region entropies exhibit diffusive fluctuations ($\sigma_q^2 \sim t$), which corresponds to the systems evolving in the EW regime, while in others they are super-diffusive ($\sigma_q^2 \sim t^{\gamma_1}$, $\gamma_1 > 1$). Before saturation the growth exponent γ_1 goes continuously form a value ≈ 1.4 for $\mu = 0.2$ to ≈ 1 for $\mu > 1$, showing the EW crossover effect, that is, the pass of a system with $t_{\text{cross}}(\mu) \ll t_s$ to $t_{\text{cross}}(\mu) \gg t_s$. In what follows we restrict our analysis to the cases with $\mu = 1$ and $\mu = 0.1$ which represent systems that for $L < 1024$ are respectively in the EW and KPZ regimes. In Fig. 6 we show the scaling of the variance of total entropies for internal and external fluctuations computed from (17) and (18). Note that in this case the interface departs from a saturated initial condition. In Fig. 7 we show the same but for the interchange entropies, computed from (13) and (14). In this case the system departs from a flat interface.

Several conclusions can be extracted from the observation of these figures.

i) The most important differences come from the kind of evolution regime. When $\mu = 1$ (EW regime) entropy fluctuations are diffusive in both growing and saturating phases of evolution, in such a way that no crossover between these phases exists. On the contrary, for the KPZ regime ($\mu = 0.1$) there exists a clear crossover between the first phase with super-diffusive entropy fluctuations and the phase of saturation with diffusive behavior. The collapse of variances for systems of distinct sizes with $t/L^{3/2}$ is a clear sign of an evolution within the KPZ regime. It is worth remarking that this behavior also occurs in the case of external fluctuations, again due to the strong dependence of such fluctuation on the internal modes.

ii) Excepting the short time behavior in Fig. 7 (a) and (c), internal and external fluctuations exhibit the same statistical behavior. The difference in this case stems from the potential term in (13) that for $\mu = 1$ is not negligible. The small differences in the scaling exponents seems to be due to the distinct degree of roughness involved in the calculation of entropies of both fluctuations.

iii) Although the dynamical scaling observed in the total and interchange entropies is very similar, there are small differences in the value of the exponents. For instance, the variance of the total entropy production in the first phase grows as $\sigma^2_{q_{\text{in}}} \sim t^{1.26} L^{1.26}$ whereas for the exchange entropy we have $\sigma^2_{r_{\text{in}}} \sim t^{1.36} L^{1.2}$. But note that we have already seen the same discrepancy with the scaling exponents in Fig. 1 when comparing cases where the initial interface is flat with others with initially correlated interfaces. Hence, the discrepancy observed in these exponents is due to the different initial conditions rather than related to the dynamics.

Conclusions. – Here, we have continued the numerical analysis of stochastic entropies in a one dimensional KPZ model initiated in [19], where only the study of stationary internal fluctuations was performed. Such a study is now extended including the analysis of external fluctuations which evolve in a non-stationary state. Moreover, we extend the parameter space studied in [19] to deal with the two possible regimes, EW and KPZ, which appear in finite systems.

Our numerical results indicate that the external fluctuations follow closely the behavior of the internal ones. This is quite a surprising result, since external fluctuations are intrinsically non-stationary and in this case the detailed fluctuation theorem, does not necessarily hold. However, the results shown in Fig.(2) indicate that for short times the theorem holds. This is because the entropy production of external fluctuations is dominated by stationary internal fluctuations. Such a dominion grows with time suggesting that the theorem should remain valid also for long times.

In our previous work we restricted our analysis to stationary cases where entropy fluctuations are almost dif-

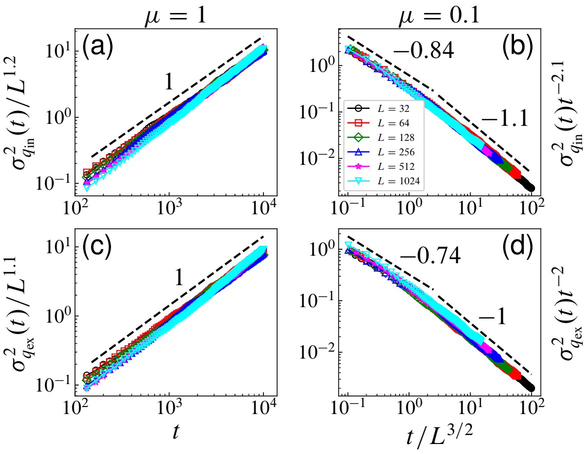

Fig. 6: Scaling of the variance of the total entropies in the EW regime, with $\mu = 1$ (panels (a) and (c)) and in the KPZ regime with $\mu = 0.1$, (panels (b) and (d)). In the figure we show the best collapse of graphs. In panels (a) and (b) we plot the entropy variance for the internal fluctuations, while in panels (c) and (d) the entropy variance of the external fluctuations is shown. Dashed straight lines with the value of the slope are added as a guide to the eye.

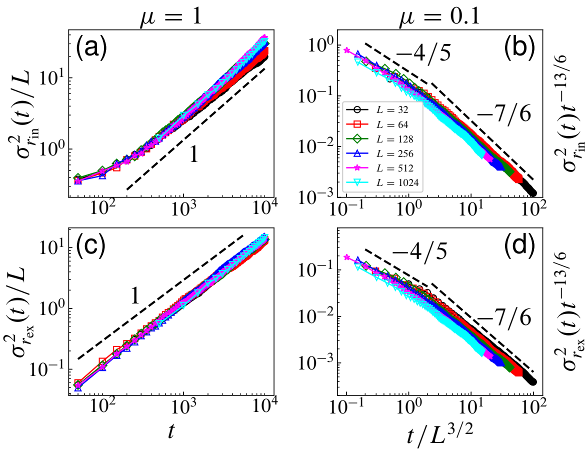

Fig. 7: Scaling of the variance of the interchange entropies for systems with flat initial conditions in the EW regime, with $\mu = 1$ (panels (a) and (c)) and in the KPZ regime with $\mu = 0.1$ (panels (b) and (d)). In panels (a) and (b) we plot the entropy variance for the internal fluctuations, while in panels (c) and (d) the entropy variance of the external fluctuations is shown. Dashed straight lines with the value of the slope are added as a guide to the eye.

fusive, that is, systems whose evolution follows the EW regime. Instead, here we have found the entropy fluctuations have super-diffusive behavior when the study is extended to cases within the KPZ regime. We then focus our work on the proper characterization of this behavior, showing how the EW to KPZ crossover involves the scaling of entropy fluctuations.

* * *

MAR and RG acknowledges support from the Ministerio de Economia y Competitividad (MINECO), Spain, under project No. Fis2016-74957-P. HSW acknowledges Financial support from Agencia Estatal de Investigación (AEI, Spain) and Fondo Europeo de Desarrollo Regional under Project PACSS (RTI2018-093732-B-C21/C22) and the Maria de Maeztu Program for units of Excellence in R&D (MDM-2817-0711).

REFERENCES

[1] Kardar M., Parisi G. and Zhang Y.-C., *Phys. Rev. Lett.*, **56** (1986) 889.
[2] Halpin-Healy T. and Zhang Y.-C., *Phys. Rep.*, **254** (1995) 215 .
[3] Barabási A. L. and Stanley H. E., *Fractal concepts in surface growth* (Cambridge University Press) 1995.
[4] Krug J. and Spohn H., in *'Kinetic roughening of growing surfaces', in Solids Far from Equilibrium*, edited by Godreche C., (Cambridge University Press) 1992.
[5] Krug J., *Advances in Physics*, **46** (1997) 139.
[6] Fogedby H. C., *Phys. Rev. Lett.*, **80** (1998) 1126.
[7] Wio H. S., Rodríguez M. A., Gallego R., Revelli J. A., Alés A. and Deza R. R., *Front. Phys.*, **4** (2017) 52.
[8] Wio H. S., *Int. J. Bifurcation Chaos*, **19** (2009) 2813.
[9] Prähofer M. and Spohn H., *Phys. Rev. Lett.*, **84** (2000) 4882.
[10] Ferrari P. L. and Spohn H., *Comm. Math. Phys.*, **265** (2006) 1.
[11] Calabrese P. and Le Doussal P., *Phys. Rev. Lett.*, **106** (2011) 250603.
[12] M. H., *arXiv:1403.6353v1 [math.PR]*, (2014) .
[13] Seifert U., *Phys. Rev. Lett.*, **95** (2005) 040602.
[14] Barato A. C., Chetrite R., Hinrichsen H. and Mukamel D., *J. Stat. Mech. Theory Exp.*, (2010) P10008.
[15] Niggemann O. and Seifert U., *J. Stat. Phys.*, **178** (2020) 1142.
[16] Niggemann O. and Seifert U., *J. Stat. Phys.*, **182** (2021) 25.
[17] Wio H. S., Rodríguez M. A. and Gallego R., *Chaos*, **30** (2020) 073107.
[18] Wio H. S., Deza R. R. and Revelli J. A., *J. Stat. Mech. Theory Exp.*, **2020** (2020) 024009.
[19] Rodríguez M. A. and Wio H. S., *Phys. Rev. E*, **100** (2019) 032111.
[20] Krug J., *Phys. Rev. A*, **44** (1991) R801.
[21] Rodríguez M. A., *Phys. Rev. E*, **90** (2014) 042122.
[22] Chernyak V. Y., Chertkov M. and Jarzynski C., *J. Stat. Mech. Theory Exp.*, **2006** (2006) P08001.
[23] To avoid unnecessary complications we always assume a pre-point time discretization of the Langevin equations, which gives a value 1 in the jacobian of the transformation $\xi \to \mathbf{y}$.
[24] Lam C.-H. and Shin F. G., *Phys. Rev. E*, **58** (1998) 5592.